

## Article

# A 24 GHz Direct Conversion Receiver for FMCW Ranging Radar Based on Low Flicker Noise Mixer

Dongze Li <sup>1,2</sup>, Qingzhen Xia <sup>1,2</sup> , Jiawei Huang <sup>1,2</sup>, Jinwei Li <sup>1,2</sup>, Hudong Chang <sup>1</sup>, Bing Sun <sup>1</sup> and Honggang Liu <sup>1,\*</sup> 

- <sup>1</sup> High-Frequency High-Voltage Device and Integrated Circuits R & D Center, Institute of Microelectronics, Chinese Academy of Sciences, Beijing 100029, China; lidongze@ime.ac.cn (D.L.); xiaqingzhen@ime.ac.cn (Q.X.); huangjiawei@ime.ac.cn (J.H.); lijinwei18@mails.ucas.edu.cn (J.L.); changhudong@ime.ac.cn (H.C.); sunbing@ime.ac.cn (B.S.)
- <sup>2</sup> School of Microelectronics, University of Chinese Academy of Sciences, Beijing 100029, China
- \* Correspondence: liuhonggang@ime.ac.cn; Tel.: +86-010-8299-5803

**Abstract:** In this paper, a 24 GHz direct conversion receiver (DCR) for frequency-modulated continuous-wave (FMCW) ranging radar based on low flicker noise mixer in 90 nm silicon-on-insulator (SOI) CMOS technology is presented. A low-noise and low-power low-noise-amplifier (LNA) adopting simultaneous noise and input matching (SNIM) method is designed. Neutralized technology and boost inductor are introduced to improve performance. The measurement results of standalone LNA show that the peak gain is 17.2 dB at 23.8 GHz and the  $-3$  dB bandwidth is around 2.2 GHz from 22.8 GHz to 25 GHz. The LNA achieves an average 3 dB NF within the 24 GHz band. A current-bleeding mixer is used to lower noise and the factors influencing flicker noise have been discussed. Proper element values and local oscillator (LO) power have been chosen to make the mixer low-noise. Measurement results illustrate that the receiver exhibits 20.3 dB peak gain, 7 dB SSB noise figure (NF) and  $-22$  dBm  $IP_{1dB}$ . Flicker noise of the mixer and the receiver are measured respectively and the noise knee-point of receiver is observed 60 kHz. The receiver consumes only 16 mW with chip area of 0.65 mm<sup>2</sup> including pads. The results demonstrate that the proposed receiver can be a promising candidate for FMCW ranging radar.

**Keywords:** receiver; 24 GHz; SOI; flicker noise; mixer; DCR; FMCW



**Citation:** Li, D.; Xia, Q.; Huang, J.; Li, J.; Chang, H.; Sun, B.; Liu, H. A 24 GHz Direct Conversion Receiver for FMCW Ranging Radar Based on Low Flicker Noise Mixer. *Electronics* **2021**, *10*, 722. <https://doi.org/10.3390/electronics10060722>

Academic Editor: Egidio Ragonese

Received: 14 February 2021

Accepted: 15 March 2021

Published: 18 March 2021

**Publisher's Note:** MDPI stays neutral with regard to jurisdictional claims in published maps and institutional affiliations.



**Copyright:** © 2021 by the authors. Licensee MDPI, Basel, Switzerland. This article is an open access article distributed under the terms and conditions of the Creative Commons Attribution (CC BY) license (<https://creativecommons.org/licenses/by/4.0/>).

## 1. Introduction

Since the Federal Communications Commission (FCC) granted unlicensed 24 GHz band as Industrial Scientific Medical (ISM) band, intense research activity toward realization of highly integrated solutions around 24 GHz band is presently underway [1]. Advances in integrated circuit and semiconductor device technologies are now enabling the development of low-cost radar products for the automotive [2], industrial [3] and consumer electronics [4]. Among them, the classical direct-conversion receiver has attracted wide-spread attention recently for its simple architecture and easy integration with the baseband circuit, as well as for its low power consumption and potentially low manufacturing costs [1].

A simplified block diagram of a DCR is illustrated in Figure 1. The echo signal is first picked up by a receiver antenna before being passed through a band select filter. The process is usually carried out in a printed circuit board (PCB). Afterwards, the signal is scaled up by a low-noise-amplifier (LNA) and is subsequently frequency down-converted by the mixer with a LO signal produced by the voltage-controlled oscillator (VCO). The LNA and mixer are key parts to complete the down-conversion operation and their performance influence subsequent detection circuit block most. In this work, the designs mainly cover the implementation and optimization of the low noise amplification and subsequent

frequency downconversion. Then, they are integrated into a low-power radar receiver radio frequency (RF) front-end.

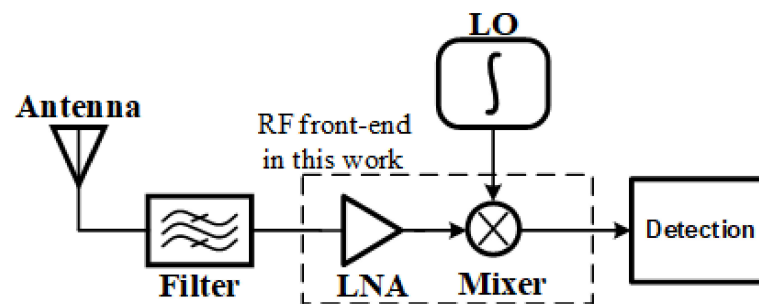


Figure 1. Simplified block diagram of DCR (direct conversion receiver).

Nevertheless, the flicker noise is the biggest obstacle in pursuing the DCR design. In millimeter-wave radars, the FMCW type has drawn the most attention because of its compact size and robustness over weather, temperature and light conditions [5–8]. However, when a DCR radar is used to measure the distance, the intermediate frequency (IF) calculated from FMCW may lie in the high flicker noise area. As shown in Figure 2, the useful baseband signal will be “buried” in noise, leading to poor measured result. A low flicker noise receiver is attractive in DCR applications. Several publications mentioned low flicker noise designs. Traditional current bleeding method was described in [9,10] and in [11] a gm-boost method was introduced with an additional circuitry connected to the switching pair transistor of the mixer to enhance gain. No measured results have been reported on 24 GHz low flicker noise receiver. In this paper, an intuitive and understandable current bleeding method is introduced to get relatively low flicker noise. Flicker noise of the mixer and the receiver are measured respectively for the first time.

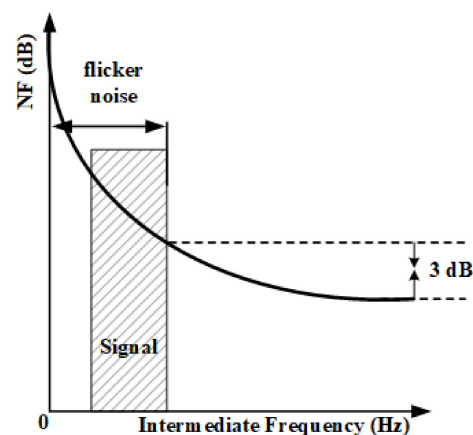


Figure 2. Baseband signal degraded by flicker noise.

The SiGe technology was once the first choice due to its excellent performance and high efficiency [2], but the low integration level and high cost are insufferable. In recent years, the burgeoning CMOS technology has become a hotspot for low-cost mm-wave radar chips [12] with its high integration and low cost. However, the lossy substrate and low-Q-factor passive components, such as inductors and capacitors, make it hard to achieve a high-gain, low-noise and low-power-consumption receiver. Compared with bulk CMOS technology, the SOI’s buried oxide layer above low resistivity substrate decreases RF coupling to the conductive silicon substrate [13]. Based on that, the SOI CMOS process is promising to overcome the weakness mentioned above. By greatly improving the circuit performance with limited increased cost, the SOI CMOS is expected to be cost-effective for good performance, low cost radar chip.

In this paper, a low noise receiver is proposed. The paper is organized as follows—in Section 2, the FMCW principle is presented. In Section 3, the low noise receiver circuit implication is described in detail. A low-noise and low-power LNA is proposed. The factors influencing flicker noise of mixer are analyzed and a low flicker noise mixer is designed. Measurement results and comparison with simulation results are shown in Section 4. Results indicate that the proposed receiver promises for 24 GHz FMCW Ranging Radar.

## 2. FMCW Principle

The principle of the FMCW ranging radar is discussed in detail here [14]. The frequency of FMCW signal changes linearly with time. A simplified model of FMCW signal can be seen in Figure 3. By calculating the frequency difference, the delay between the transmitted wave and the reflected wave can be known to determine the position of the target. It can be expressed as

$$R = \frac{c \cdot T \cdot f_r}{2B} \quad (1)$$

where  $R$  stands for the distance between target and radar,  $c$  is the speed of light,  $T$  is the duration of the chirp,  $f_r$  is the beat frequency and  $B$  is the bandwidth of carrier frequency.

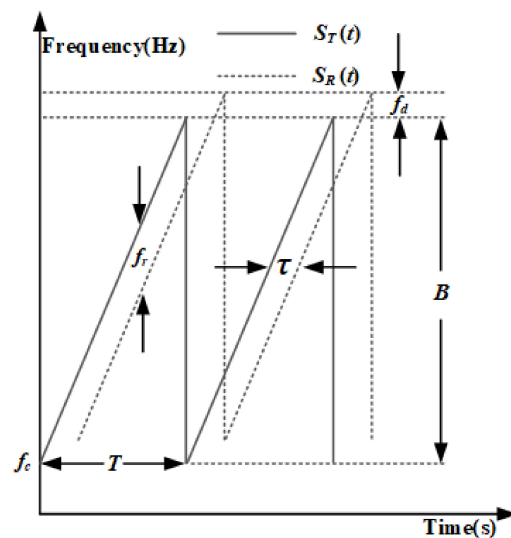


Figure 3. FMCW (frequency-modulated continuous-wave) principle of a sawtooth wave.

As mentioned above, the beat frequency  $f_r$  goes linearly with distance  $R$ . If the target is relatively close to the radar, the  $R$  is small; thus, the beat frequency  $f_r$  is also small. For example, when the distance between radar and target is 3 m,  $B$  is 250 MHz and  $T = 0.5$  ms is a regular resolution. Thus, the calculated 10 kHz beat frequency  $f_r$  is lying in the high flicker noise area exactly. As a consequence, the short-range detecting ability deteriorates.

The beat frequency containing information of target is calculated from received RF signal and LO signal and it is irrelevant to the received signal scope. In this way, the receiver used for FMCW can loosen restriction of linearity.

## 3. Circuit Implementations

Figure 4 shows the proposed direct down-conversion receiver with dimensions of the RF active devices. The passive element values of proposed circuit are shown in Table 1. These element values are based on the results of EM simulation. The receiver is based on the zero IF architecture with RF and LO signals operating in the 24 GHz frequency band. Low noise, low power consumption and high integration are some of the important system requirements of the receiver. To avert lossy balun and reduce the power consumption of this circuit, single-end topology is used.  $L_{d2}$  was the load of LNA and its inductance was chosen to form the matching circuit with  $C_{p2}$  and  $L_{p2}$  between the output of LNA

and input of mixer. The LO input ports of the mixer were matched to  $50\ \Omega$  impedance by introducing the matching inductors  $L_{p3}$  and  $L_{p4}$ .

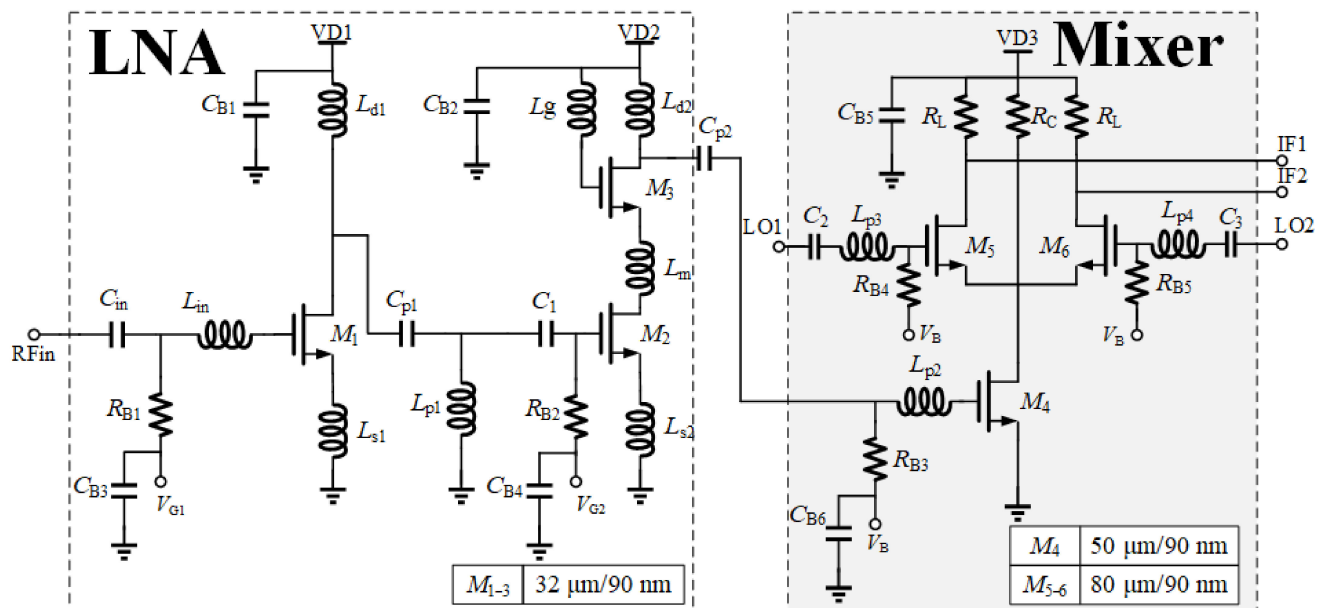


Figure 4. Schematic of proposed receiver.

Table 1. Values of the circuit elements of the proposed receiver.

$C_{in}$	$C_{B1-6}$	$C_{p1}$	$C_{p2}$	$C_{1-3}$	$L_{in}$	$L_{s1}$	$L_{s2}$	$L_{d1}$
1.25 pF	2 pF	200 fF	550 fF	1 pF	720 pH	300 pH	270 pH	600 pH
$L_{d2}$	$L_m$	$L_g$	$L_{p1}$	$L_{p2}$	$L_{p3-4}$	$R_{B1-5}$	$R_L$	$R_C$
450 pH	130 pH	150 pH	180 pH	300 pH	430 pH	1.2 k $\Omega$	800 $\Omega$	60 $\Omega$

According to the system noise cascading formula, to keep the whole system low noise, LNA as the first stage should have enough gain and low noise [15]. The mixer used for down-converting RF signals should keep low flicker noise. Detailed design methods are described in following parts.

### 3.1. LNA Design

As depicted in Figure 4, a two-stage single-end LNA is designed in our work. The first stage plays the key part in the noise figure of the system. To meet the requirements of noise figure and gain, a common-source (CS) amplifier is set to be first stage to keep the circuit low-noise, followed by a cascode amplifier to enhance gain. SNIM method [16] was introduced in this design to ensure high gain and low NF without sacrificing each other, which used to be a tradeoff. As shown in Figure 4,  $L_{s1}$  and  $L_{s2}$  worked as source degeneration inductors to simplify the LNA's input and noise matching. The researcher in [13] reported that the SNIM state will be easily influenced by the bias circuit when designing LNAs, leading to mismatch and deteriorated performance. Based on simulated results, a 1200  $\Omega$  resistor was chosen in the bias circuit and the bias circuit was placed proposition before  $L_{in}$ . The input port of the LNA is matched to  $50\ \Omega$  impedance. In receiver the output port of the LNA is matched to mixer and in standalone LNA the output port of the LNA is matched to  $50\ \Omega$  impedance.

To reduce the power consumption as much as possible, bias voltage of amplificatory transistors is elaborately set to 0.55 V for enough gain, acceptable NF and power consumption. Moreover, sizes of transistors  $M_1$ ,  $M_2$  and  $M_3$  were selected elaborately through simulation.  $L_m$ , as neutralized inductor, was added between the CS and the common-gate

(CG) transistors to resonate with parasitic capacitor to minimize the NF and increase the gain [15]. Meantime, an inductor  $L_g$  was added at the gate of the CG transistor as resonant tank to boost gain at the target frequency [17].  $L_m$  was well-designed transmission line fabricated with upmost metal to maintain high  $Q$ , as well as  $L_g$ . A matching network composed of  $C_{p1}$ ,  $L_{p1}$  and  $C_1$  is used to get interstage match.  $C_{B1}$ – $C_{B4}$  are bypass capacitors for leaching the clutter signal from supply source.

### 3.2. Low Flicker Noise Mixer Design

In general, the mixer flicker noise shown in and flicker noise figure shown in Equations (2) and (3) are [18]:

$$V_{n,out}(f) = \frac{8I_{ss}f_{LO}}{S_{LO}} R_l \cdot V_{n,LO}(f) \quad (2)$$

$$NF(1/f) = 1 + \frac{\pi^2 \frac{8I_{ss}f_{LO}}{S_{LO}} \cdot V_{n,LO}(f)}{4g_m^2 R_l} \cdot \frac{1}{4kTR_s} \quad (3)$$

where  $I_{ss}$  is the DC current flowing through each pair of  $LO$  switch transistor;  $k$  is Boltzmann constant;  $f_{LO}$  is frequency of  $LO$  signal;  $S_{LO}$  is the slope of the differential  $LO$  wave form;  $V_{n,LO}(f)$  is flicker noise of switch transistor;  $g_m$  is gm of amplifying transistor;  $R_l$  is load resistance;  $R_s$  is the source resistance. From equations above, smaller  $I_{ss}$  and higher  $S_{LO}$  help to decrease the flicker noise, so long as other parameters stay unchanged. In this design, reducing the  $I_{ss}$  and enlarging the  $S_{LO}$  are considered to reduce the flicker noise of the mixer.

A conventional single-balanced mixer is shown in Figure 5a,b shows a single-balanced mixer with current-bleeding technology. For a conventional single-balanced mixer, as shown in Figure 5a, transistor  $M_1$  acts as the driver-stage to convert the input RF voltage into current signals and transistors  $M_{2-3}$  are biased at near pinch-off region to act as switches and steer the current depending on the  $LO$  signal.

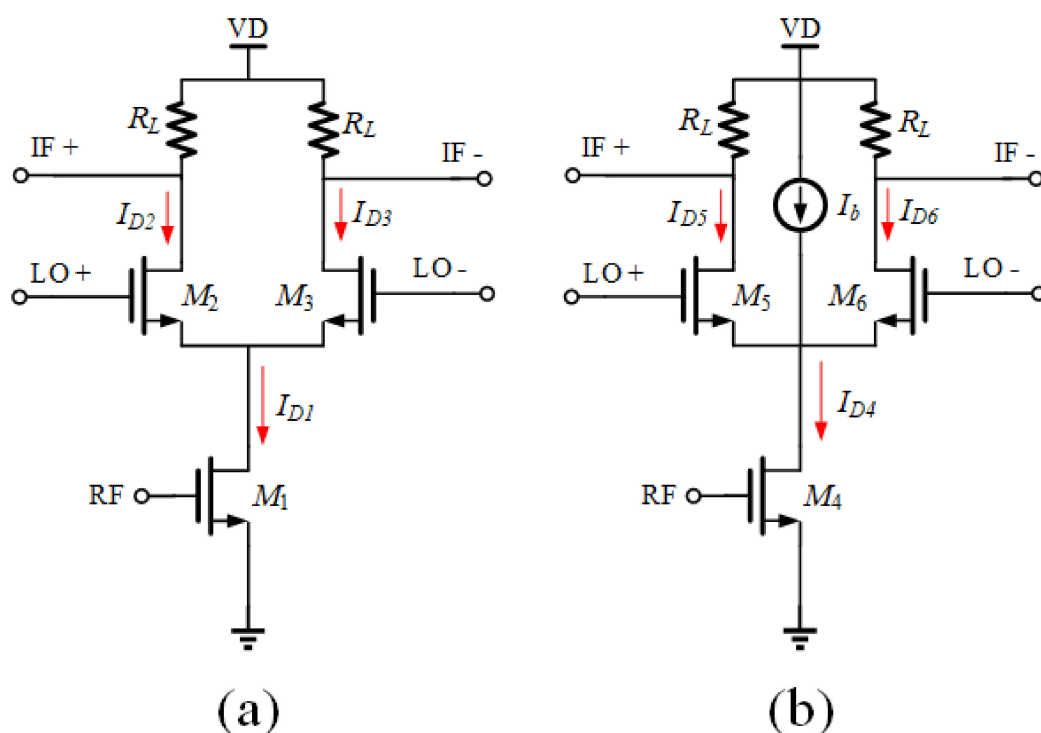


**Figure 5.** (a) Conventional single-balanced mixer; (b) single-balanced mixer with current-bleeding technology.

From Figure 5a, the driver-stage current  $I_{D1}$  is equal to switch-stage current  $I_{D2}$  plus  $I_{D3}$ . Increasing in the driver stage current ( $I_{D1}$ ) forces the reduction of load resistance  $R_L$  to

maintain the fixed DC working state, degrading conversion gain of the mixer. Furthermore, large current at switch-stage leads to high noise [19]. Therefore, at that case, current-bleeding technology is introduced. In Figure 5b, the driver-stage current  $I_{D4}$  is equal to switch-stage current including  $I_{D2}$  and  $I_{D3}$  plus bleeding current  $I_b$ . In other words, current bleeding allows the control of the DC current for the switching transistors separately from that of the driver-stage. By these means,  $I_{D4}$  can be higher than  $I_{D5} + I_{D6}$  and switch-stage current can be lowered to reduce the flicker noise of proposed mixer.

Assuming the driver-stage current  $I_{D1}$  in Figure 5a is equal to the driver-stage current  $I_{D4}$  in Figure 5b. Based on Equation (2), the mixer flicker noise in Figure 5a,b can be expressed as:

$$V_{n,out}(f)_a = \frac{4I_{D1}f_{LO}}{S_{LO}}R_L \cdot V_{n,LO}(f) \quad (4)$$

$$V_{n,out}(f)_b = \frac{4(I_{D1} - I_b)f_{LO}}{S_{LO}}R_L \cdot V_{n,LO}(f) \quad (5)$$

Because of the bleeding current  $I_b$ , flicker noise in Equation (5) is smaller than that in Equation (4). In this way, the flicker noise with current-bleeding structure in Figure 5b promises smaller than that with conventional structure in Figure 5a.

Referred to Figure 4, the proposed mixer adopted a resistor  $R_C$  as a bleeding current source. Resistances of load resistor  $R_L$  and bleeding source resistor  $R_C$  are selected by elaborate simulation to keep good performance. In the design,  $R_C$  was chosen to be 60  $\Omega$  and load resistor was 800  $\Omega$ . The analysis on the mixer of static operating point shows that the bleeding current  $I_b$  takes 97% of whole DC current  $I_{D4}$ . The drain voltages of  $M_4$ ,  $M_5/M_6$  are 0.5 V and 1.1 V. The voltage drop of load resistor  $R_L$  is 0.1 V, making sure the headroom of this design under a 1.2 V supply voltage. However, the small resistance of  $R_C$  caused conversion gain loss to a certain extent. The simulation result showed that signal power loss caused by  $R_C$  was about 70%, leading to about 5 dB conversion gain loss.

Based on the bleeding-current mixer, simulation was carried out on different LO power to find a suitable one to achieve low flicker noise. Result is depicted in Figure 6, showing that flicker noise is decreasing with LO power increasing. The result is in accord with Equation (3). From Figure 6, the LO power is increasing from  $-15$  dBm to 0 dBm. Larger LO power was not adopted, because the 24 GHz frequency source could only offer moderate LO power in a system, for example,  $-10$  dBm. Larger LO power needs additional amplifiers and power consumption, making system not cost-efficient. At last, a 0 dBm LO power was chosen.

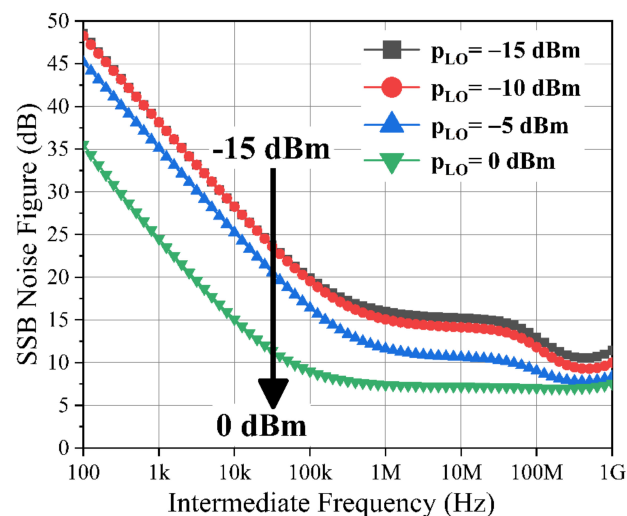


Figure 6. Simulated flicker noise of mixer with different LO (local oscillator) power.

#### 4. Results

The 90 nm SOI CMOS technology has been utilized in this work for the receiver realization. The technology features five metal layers with two thick RF metals on the top. The upper two RF metal layers with 3.3  $\mu\text{m}$  thickness have been extensively utilized for the realization of on-chip transmission lines and spiral inductors. The design benefited from the high resistivity of the SOI substrate; thus, the traditional patterned ground shields on the bottom of on-chip spiral inductors could be omitted. High-Q inductors and capacitors can be realized. In addition, all the critical on-chip interconnections are based on the shielded co-planar transmission line structures. Taking into consideration the influence of electromagnetic coupling between lines and passive components, elaborate and complete EM simulation was carried out to ensure the accuracy of this design.

Figure 7 shows the micrograph of the realized receiver circuit. Decoupling capacitors with 2 pF capacitance were placed between every DC pad and closest ground pad to filter clutter from DC sources. The compact receiver chip achieves a total chip area (including the pads) of 0.65 mm<sup>2</sup> (1 mm  $\times$  0.65 mm). Test chips for two main building blocks namely the LNA and mixer have also been integrated on separate dies and tested alone. Standalone LNA and mixer occupy 0.16 mm<sup>2</sup> and 0.18 mm<sup>2</sup>, respectively. Chips have been bonded on PCB for characterization. All RF signals have been provided through probe station. Small-signal measurements were carried out with Agilent N5247A network analyzer. The Agilent N8975A NFA offered platform for NF measurements.

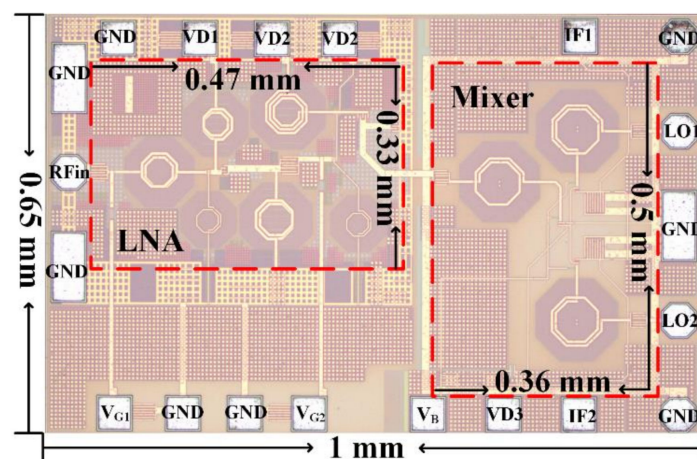
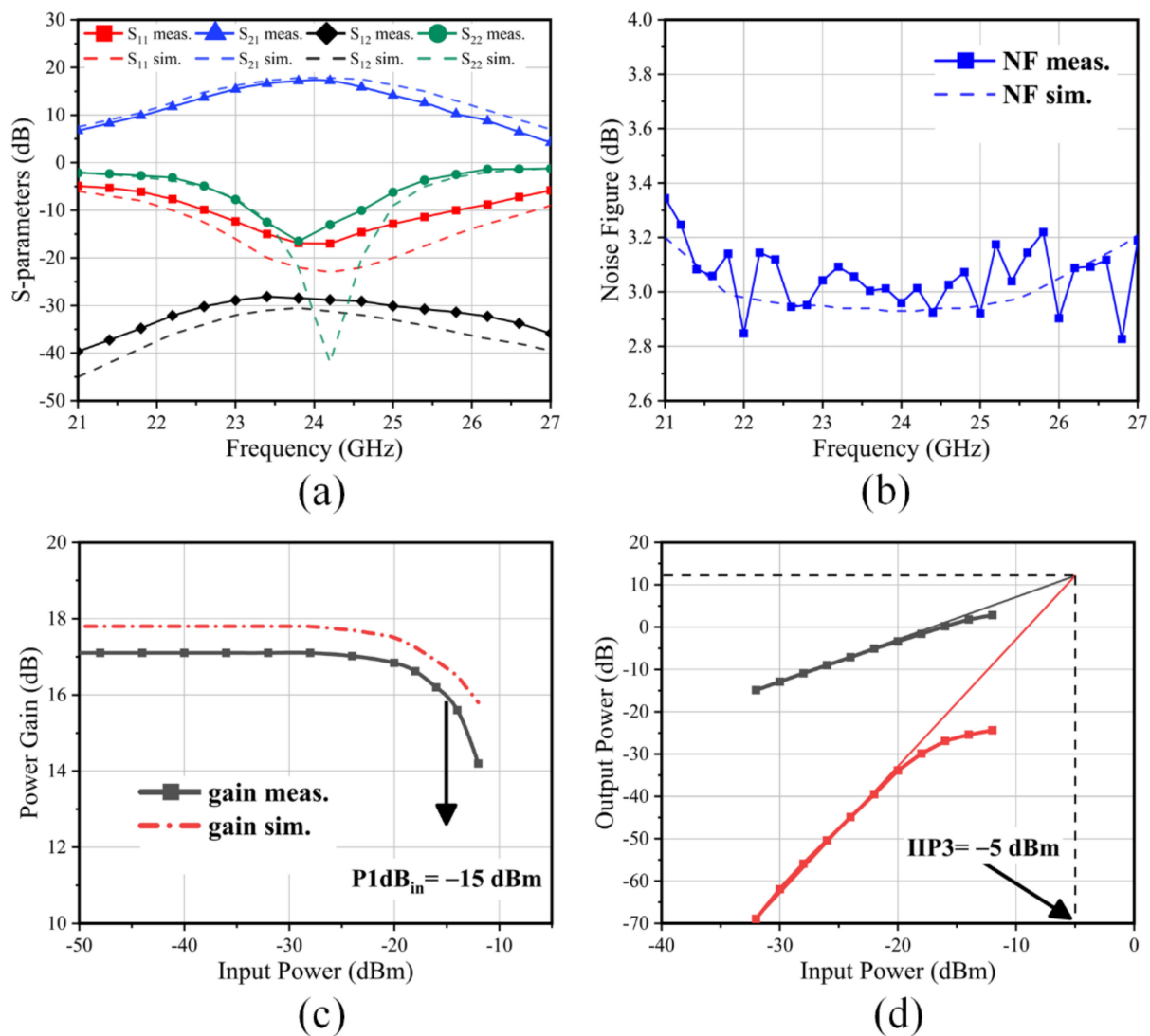


Figure 7. Chip photo of the proposed receiver.

Performance of the LNA has been presented in Figure 8. The measured and simulated small-signal S-parameters, NF,  $P_{1\text{dB}}$  and  $IIP_3$  of LNA are depicted in Figure 8a–d, separately. The measured  $S_{21}$  reached 17.2 dB of its peak at 23.8 GHz and the  $-3$  dB bandwidth is around 2.2 GHz from 22.8 GHz to 25 GHz. Compared with simulation results, the deteriorated  $S_{11}$  and  $S_{22}$  worsen gain and bandwidth. The  $S_{11}$  is lower than  $-10$  dB from 22.5 GHz to 26.6 GHz and  $S_{22}$  is under  $-10$  dB from 23.2 GHz to 24.6 GHz. The parameter standing for isolation from output to input  $S_{12}$  is below  $-30$  dB within the whole working band. The results in Figure 8b show that the LNA achieves an average 3 dB NF within the 24 GHz band. The linearity performance is illustrated in Figure 8c,d. Figure 8c plots the power gain versus input power and the  $IP_{1\text{dB}}$  could be observed  $-15$  dBm. The  $IIP_3$  is found to be  $-5$  dBm in Figure 8d.



**Figure 8.** (a) S-parameters of LNA (low-noise-amplifier); (b) NF (noise figure) of LNA; (c)  $P_{1dB}$  of LNA; (d)  $IIP_3$  of LNA.

A second set of experiments was carried out on the receiver including LNA and mixer. Another signal source has been introduced to feed the 0 dBm LO signal to mixer. The measurements were carried out by sweeping the RF and LO frequency with fixed IF of 125 MHz. Figure 9 presents the measured and simulated results of the receiver chip. Figure 9a shows the simulated and measured conversion gain and noise figure performance of the receiver and 20.3 dB gain and 7 dB SSB NF are achieved. Compared with the simulation results, with influence of parasitic part and test environment, the measured conversion gain is 3.5 dB lower and the NF is 1 dB higher. The  $-3$  dB bandwidth of receiver is constrained mainly by LNA, which is 2.2 GHz from 22.8 GHz to 25 GHz as well. Shown in Figure 9b is the RF and LO matching performance of the receiver. Even though measured results are worse than simulated results, the  $S_{11}$  is below  $-10$  dB from 23 GHz to 27 GHz and  $S_{22}$  is below  $-10$  dB from 23.2 GHz to 25.4 GHz. It means that RF port and LO port input match well, respectively. The port-to-port isolation has been characterized for proposed receiver from 21 GHz to 27 GHz and shown in Figure 9c. All the isolation levels are more than 30 dB in 24 GHz band. The LO-IF isolation is much lower, because the LO signal is fed directly to the mixer with relatively higher amplitude. With 24 GHz RF and 125 MHz IF, the input power at 1 dB gain compression point value of  $-22$  dBm has been measured in Figure 9d.

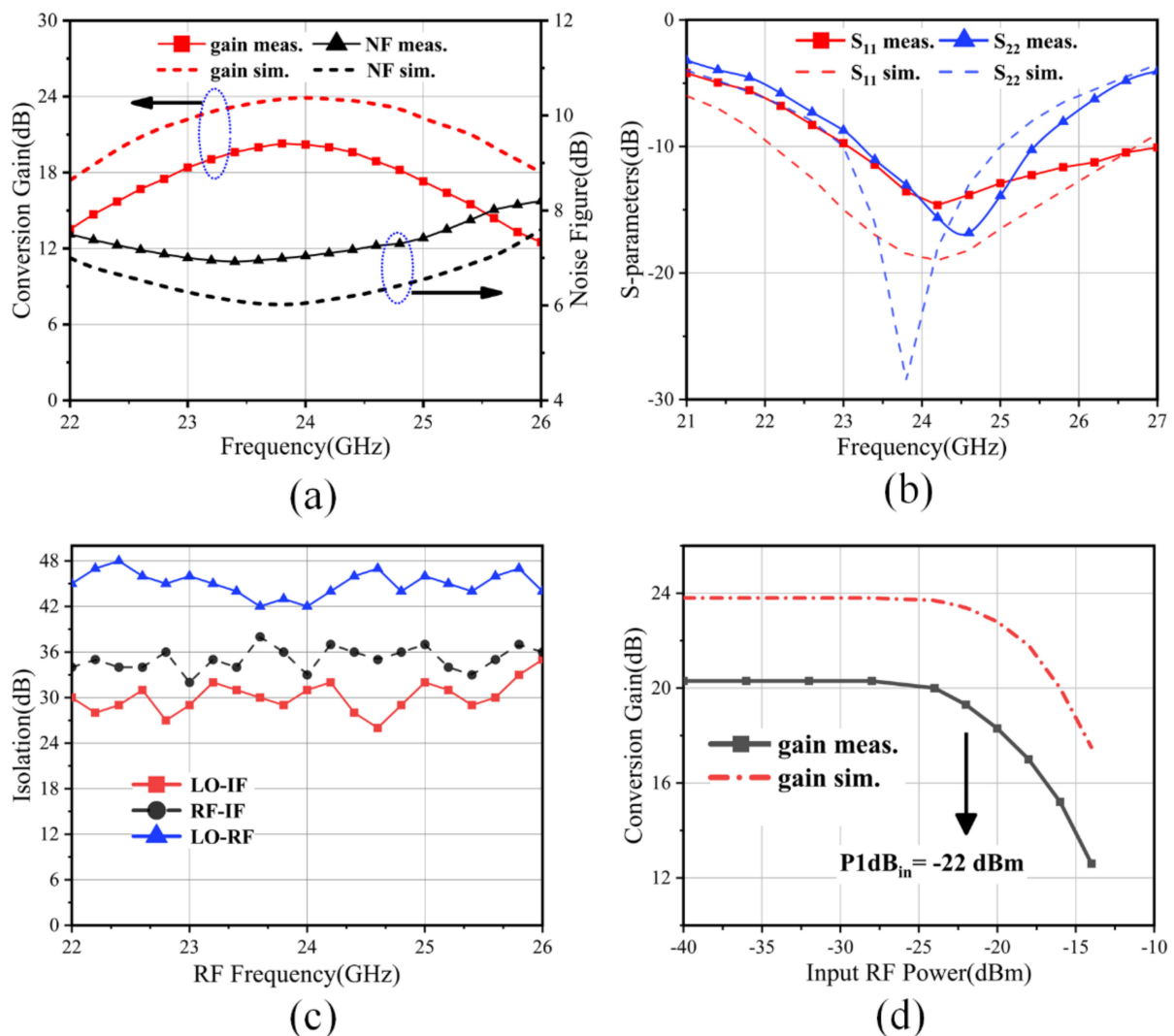


**Figure 9.** (a) Conversion gain and NF (noise figure) of receiver; (b) S-parameters of RF (radio frequency) and LO (local oscillator) ports; (c) Measured port isolation of receiver; (d)  $P_{1dB}$  of receiver.

Measured flicker noise results of standalone mixer and receiver are shown in Figure 10. To verify influence of LO power on flicker noise, two LO power are set to  $-10$  dBm and  $0$  dBm. The IF is selected from  $100$  Hz to  $10$  MHz and log scale is used to make results clear and intuitive. The results indicate that larger LO power can reduce the flicker noise of receiver, same as the simulated results. From Figure 10a, the flicker noise of mixer is higher than above simulation result. The reason may be inexact noise model of transistor and loss introduced by measure equipment. The literature often uses the term “knee-point” for the frequency below which the flicker noise dominates over thermal noise. Commonly, we consider the frequency at which the noise figure is  $3$  dB higher than the lowest noise figure to be knee-point. With a  $0$  dBm LO power, the knee-point is observed to be  $60$  kHz. Compared with the  $48$  kHz ideal simulated knee-point reported in [18], this circuit achieved a relatively low noise corner. In Figure 10b, because of the former-stage high-gain LNA, the contribution about NF of mixer part has been reduced. Then, a relatively low noise is achieved. Furthermore, as shown in Figure 10, noise under two different LO power stays almost the same when IF is larger than  $100$  kHz. With parameters in Equation (1),  $100$  kHz IF results from  $30$  m target distance. In a real scenario, when the target distance is larger than  $30$  m, a lower LO power can be used to save power consumption whilst introducing no more noise.

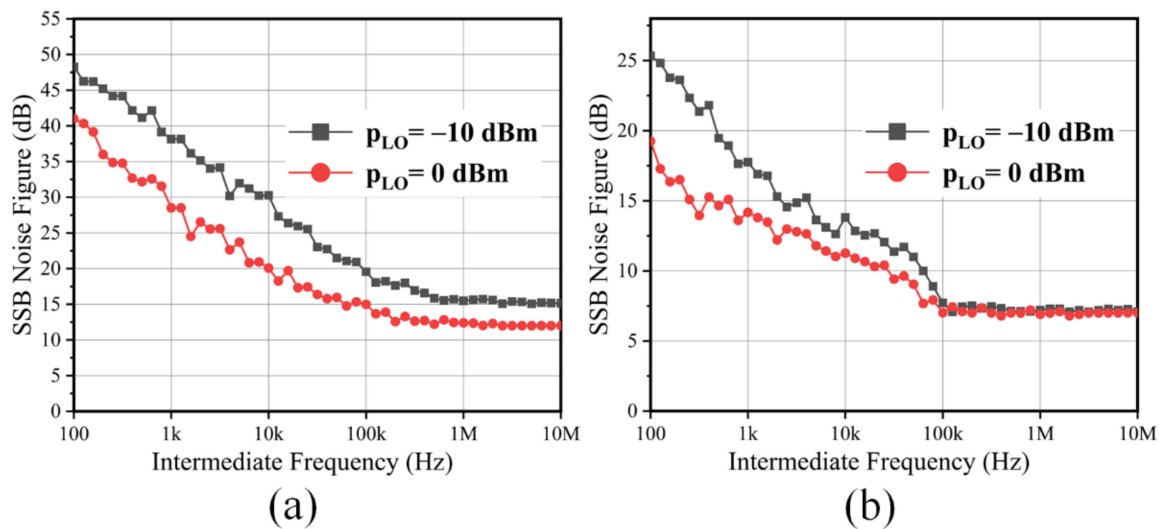


Figure 10. (a) Flicker noise results of mixer; (b) flicker noise results of receiver.

Table 2 compares the realized receiver performance with the published state-of-art K-band receivers. From this comparison, it can be seen that the realized 24 GHz CMOS receiver compares the state-of-the-art realizations with a balanced performance even in a non-superior process. The gain is not so high as [20] because high-gain variable-gain amplifier (VGA) can be integrated in later design easily. This design achieves a knee-point of 60 kHz. It's the first time to report a low flicker noise measured result. In order to distinguish the power consumption of bias circuit is included or not, the  $P_{DC}$  part has been divided into two lines:  $P_{DC1}$  and  $P_{DC2}$ . The former stands for the power consumption including the bias circuit and the latter stands for the power consumption excluding the bias circuit. As talked above, the linearity restriction can be loosened in FMCW application, so the  $-22$  dBm IP1dB is adequate.

Table 2. Performance comparison table.

	This Work	[20]	[21]	[22]	[23] <sup>1</sup>
Technology	90 nm SOI	0.13 $\mu$ m CMOS	65 nm CMOS	65 nm CMOS	45 nm SOI
Inclusion	LNA + Mixer	LNA + Mixer + VGA	LNA + Mixer	LNA + Mixer	LNA + Mixer
RF/IF (GHz)	24/0.125	24/0.1	24/0.002	21.5/0.1	24/NA
CG (dB)	20.3	36	28.3	14.5	26.2
NF (dB)	7	9.9	5	5.7	5.6
IP <sub>1dB</sub> (dBm)	$-22$	$-35$	$-28$	$-40$	NA
Knee-point (kHz)	60	NA	NA	NA	NA
$P_{DC1}$ (mW)	21.1 <sup>1</sup>	40.8	26	NA	NA
$P_{DC2}$ (mW)	16	NA	NA	0.683	NA
Area <sup>2</sup> (mm <sup>2</sup> )	0.65	0.8	0.66	0.4	NA

<sup>1</sup> simulation results; <sup>2</sup> including pads.

## 5. Conclusions

In this paper, a low-noise 24 GHz direct conversion receiver for FMCW ranging radar is designed and fabricated in 90 nm SOI CMOS technology. A low-noise and low-power LNA is proposed. To enhance gain of the receiver and reduce NF, the SNIM method was used in the input. Neutralized technology and boost inductors were introduced to improve performance. A 24 GHz current-bleeding mixer was introduced and the factors influencing flicker noise have been discussed. The measured results show the proposed receiver exhibits 20.3 dB peak gain and 7 dB SSB NF. A  $-22$  dBm IP1dB and well-matched RF port S11 and LO port S22 have been measured. More than 30 dB isolations between RF, LO and IF ports are obtained within working frequency band. Flicker noise of both mixer

and receiver are measured and the knee point of receiver is observed 60 kHz. Combined with the FMCW principle, the receiver indicates when the target distance is larger than 30 m, a lower LO power can be used to save power consumption. The receiver consumes only 16 mW with chip area of 0.65 mm<sup>2</sup> including pads. It suggests that the proposed SOI CMOS DCR receiver can be a promising candidate for FMCW ranging radar.

**Author Contributions:** Conceptualization, D.L.; methodology, Q.X.; software, J.H.; validation, J.L.; resources, H.C.; writing—review and editing, B.S.; project administration, H.L. All authors have read and agreed to the published version of the manuscript.

**Funding:** This work was supported by the National Key Research and Development Program of China under Grant No. 2016YFA0202304 and 2016YFA0201903, General Program of National Natural Science Foundation of China under Grant No.61674168 and 61504165, as well as the Opening Project of Key Laboratory of Microelectronics Devices and Integrated Technology, Institute of Microelectronics, Chinese Academy of Sciences.

**Acknowledgments:** The authors would like to thank Yankui Li for the measurement support.

**Conflicts of Interest:** The authors declare no conflict of interest. The funders had no role in the design of the study; in the collection, analyses, or interpretation of data; in the writing of the manuscript, or in the decision to publish the results.

## References

1. Mazzanti, A.; Sosio, M.; Repposi, M.; Svelto, F. A 24 GHz Subharmonic Direct Conversion Receiver in 65 nm CMOS. *IEEE Trans. Circuits Syst. I Regul. Pap.* **2010**, *58*, 88–97. [[CrossRef](#)]
2. Ragonese, E.; Scuderi, A.; Giannello, V.; Messina, E.; Palmisano, G. A fully integrated 24GHz UWB radar sensor for automotive applications. In Proceedings of the 2009 IEEE International Solid-State Circuits Conference—Digest of Technical Papers, San Francisco, CA, USA, 8–12 February 2009; pp. 306–307. [[CrossRef](#)]
3. Subramanian, V.; Zhang, T.; Boeck, G. Low Noise 24 GHz CMOS Receiver for FMCW Based Wireless Local Positioning. *IEEE Microw. Wirel. Compon. Lett.* **2011**, *21*, 553–555. [[CrossRef](#)]
4. Evans, R.J.; Farrell, P.M.; Felic, G.; Duong, H.T.; Le, H.V.; Li, J.; Li, M.; Moran, W.; Morelande, M.R.; Skafidas, E. Consumer radar: Technology and limitations. In Proceedings of the International Conference on Radar, Adelaide, Australia, 9–12 September 2013; pp. 21–26. [[CrossRef](#)]
5. Park, J.; Ryu, H.; Ha, K.-W.; Kim, J.-G.; Baek, D. 76–81-GHz CMOS Transmitter With a Phase-Locked-Loop-Based Multichirp Modulator for Automotive Radar. *IEEE Trans. Microw. Theory Tech.* **2015**, *63*, 1399–1408. [[CrossRef](#)]
6. Luo, T.-N.; Wu, C.-H.E.; Chen, Y.-J.E. A 77-GHz CMOS Automotive Radar Transceiver With Anti-Interference Function. *IEEE Trans. Circuits Syst. I Regul. Pap.* **2013**, *60*, 3247–3255. [[CrossRef](#)]
7. Ginsburg, B.P.; Subburaj, K.; Samala, S.; Ramasubramanian, K.; Singh, J.; Bhatara, S.; Murali, S.; Breen, D.; Moallem, M.; Dandu, K.; et al. A multimode 76-to-81GHz automotive radar transceiver with autonomous monitoring. In Proceedings of the 2018 IEEE International Solid-State Circuits Conference—(ISSCC), San Francisco, CA, USA, 11–15 February 2018; pp. 158–160. [[CrossRef](#)]
8. Dudek, M.; Nasr, I.; Bozskik, G.; Hamouda, M.; Kissinger, D.; Fischer, G. System Analysis of a Phased-Array Radar Applying Adaptive Beam-Control for Future Automotive Safety Applications. *IEEE Trans. Veh. Technol.* **2015**, *64*, 34–47. [[CrossRef](#)]
9. Wei, P.; Diao, S.; Huang, D.; Fu, Z.; Lin, F. A K-Band Down-Conversion mixer design with integrated baluns in 65nm CMOS. In Proceedings of the Proceedings of 2012 5th Global Symposium on Millimeter-Waves, Harbin, China, 27–30 May 2012; pp. 282–285. [[CrossRef](#)]
10. Ali, M.K.; Hamidian, A.; Malignaggi, A.; Arnous, M.T.; Boeck, G. Low flicker noise high linearity direct conversion mixer for K-band applications in a 90 nm CMOS technology. In Proceedings of the 2014 20th International Conference on Microwaves, Radar and Wireless Communications (MIKON), Gdańsk, Poland, 16–18 June 2014; pp. 1–4. [[CrossRef](#)]
11. Ahn, D.; Kim, D.-W.; Hong, S. A K-Band High-Gain Down-Conversion Mixer in 0.18  $\mu\text{m}$  CMOS Technology. *IEEE Microw. Wirel. Compon. Lett.* **2009**, *19*, 227–229. [[CrossRef](#)]
12. Krishnaswamy, H.; Hashemi, H. A Fully Integrated 24GHz 4-Channel Phased-Array Transceiver in 0.13  $\mu\text{m}$  CMOS Based on a Variable-Phase Ring Oscillator and PLL Architecture. In Proceedings of the IEEE International Solid-State Circuits Conference. Digest of Technical Papers, San Francisco, CA, USA, 11–15 February 2007; pp. 124–591. [[CrossRef](#)]
13. Li, D.; Xia, Q.; Huang, J.; Li, J.; Chang, H.; Sun, B.; Liu, H. A 4-mW Temperature-Table 28 GHz LNA with Resistive Bias Circuit for 5G Applications. *Electronics* **2020**, *9*, 1225. [[CrossRef](#)]
14. Ma, T.; Deng, W.; Chen, Z.; Wu, J.; Zheng, W.; Wang, S.; Qi, N.; Liu, Y.; Chi, B. A CMOS 76–81-GHz 2-TX 3-RX FMCW Radar Transceiver Based on Mixed-Mode PLL Chirp Generator. *IEEE J. Solid-State Circuits* **2019**, *55*, 233–248. [[CrossRef](#)]
15. Huang, B.-J.; Lin, K.-Y.; Wang, H. Millimeter-Wave Low Power and Miniature CMOS Multicascade Low-Noise Amplifiers with Noise Reduction Topology. *IEEE Trans. Microw. Theory Tech.* **2009**, *57*, 3049–3059. [[CrossRef](#)]

16. Nguyen, T.-K.; Kim, C.-H.; Ihm, G.-J.; Yang, M.-S.; Lee, S.-G. CMOS Low-Noise Amplifier Design Optimization Techniques. *IEEE Trans. Microw. Theory Tech.* **2004**, *52*, 1433–1442. [[CrossRef](#)]
17. Yu, Z.; Feng, J.; Guo, Y.; Li, Z. Analysis and design of a V-band low-noise amplifier in 90 nm CMOS for 60 GHz applications. *IEICE Electron. Express* **2015**, *12*. [[CrossRef](#)]
18. Kong, Y.; Yan, N. High gain and low flicker noise down-conversion mixer applied in 24GHz FMCW radar. In Proceedings of the 2018 IEEE MTT-S International Wireless Symposium (IWS), Chengdu, China, 6–10 May 2018; pp. 1–4. [[CrossRef](#)]
19. Lai, D.; Chen, Y.; Wang, X.; Chen, X. A CMOS Single-Differential LNA and current bleeding CMOS mixer for GPS Receivers. In Proceedings of the 2018 2010 IEEE 12th International Conference on Communication Technology, Nanjing, China, 11–14 November 2010; pp. 677–680. [[CrossRef](#)]
20. Wang, H.; Jiao, C.; Zhang, L.; Zeng, D.; Yang, D.; Wang, Y.; Yu, Z. A low-power ESD-protected 24GHz receiver front-end with  $\pi$ -type input matching network. In Proceedings of the 2011 IEEE International Symposium of Circuits and Systems (ISCAS), Rio de Janeiro, Brazil, 15–18 May 2011; pp. 2877–2880. [[CrossRef](#)]
21. Cheng, J.; Hsieh, C.; Wu, M.; Tsai, J.; Huang, T. A 0.33 V 683 uw K-Band Transformer-Based Receiver Front-End in 65 nm CMOS Technology. *IEEE Microw. Wirel. Compon. Lett.* **2015**, *25*, 184–186. [[CrossRef](#)]
22. Ding, Y.; Vehring, S.; Maurath, D.; Gerfers, F.; Boeck, G. A 24 GHz Zero-IF IQ-receiver using low-noise quadrature signal generation. In Proceedings of the 2017 IEEE Asia Pacific Microwave Conference (APMC), Kuala Lumpur, Malaysia, 13–16 November 2017; pp. 1226–1229. [[CrossRef](#)]
23. Wang, Y.; Cui, J.; Zhang, R.; Sheng, W. Fully differential Ultra-wideband LNA-Mixer for K to Ka Band receiver in 45nm CMOS SOI technology. In Proceedings of the 2019 IEEE Asia-Pacific Microwave Conference (APMC), Singapore, 10–13 December 2019; pp. 16–18. [[CrossRef](#)]